Crystal structure of $Sr_{0.875}Nd_{0.125}CuO_{2-\delta}$ superconducting thin films

Nobuyuki Sugii and H. Yamauchi
Superconductivity Research Laboratory, International Superconductivity Technology Center, 1-10-13 Shinonome, Koto-ku, Tokyo 135, Japan

Mitsuru Izumi
Department of Physics, Tokyo University of Mercantile Marine, 2-1-6, Etchujima, Koto-ku, Tokyo 135, Japan
(Received 15 February 1994; revised manuscript received 1 June 1994)

The crystal structure of $Sr_{0.875}Nd_{0.125}CuO_{2-\delta}$ superconducting thin film was determined by x-ray diffraction. The intensity data were collected by four-circle x-ray diffractometry and the absorption correction for a thin platelike crystal of 780 Å thick was made. The structure was found to belong to space group $P4/mmm$ with $a=3.920(1)$ Å, $c=3.418(1)$ Å, and $Z=1$, which is almost identical with that of $Ca_{0.84}Sr_{0.16}CuO_2$. The Cu-O coordination was found to be square planar without detectable buckling of the plane and no apical oxygen ions were observed. The occupation factors of Sr and Nd were slightly less than the nominal ones. The anisotropic thermal parameters for Sr, Nd, and Cu ions were elongated along the c direction, indicating the crystallographical two dimensionality of the infinite-layer structure.

I. INTRODUCTION

The basic structural feature of superconducting cuprates is the existence of planar copper-oxygen sheets. The oxygen ion coordination around a copper ion is thought to be one of the most important factors to control the electronic structure and other physical properties of these compounds. As so-called infinite-layer cuprates have a crystal structure in which the corners of the CuO_4 squares are shared,[1] they are thought to be suitable cuprates for the study of the role of copper-oxygen sheets in the mechanism of superconductivity.

Superconducting cuprates having an infinite-layer structure, such as $Sr_{1-x}Nd_xCuO_{2-\delta}$, can be synthesized by high-pressure synthesis techniques[2] or vapor-deposition techniques.[3,4] Unfortunately, single crystals of these compounds have not yet been obtained. Therefore, epitaxially grown thin films are considered to be single crystals employed for the investigation of physical properties of the compounds. The crystal structure provides basic information for understanding the physical properties. However, there has been little information about the crystal structures of thin films because of the difficulty in determining them.

In this study, we determined the crystal structure of $Sr_{1-x}Nd_xCuO_{2-\delta}$ superconducting thin film using the intensity data collected by four-circle x-ray diffractometery. In the analysis, the absorption correction for the thin platelike crystal was performed and the crystal structure was refined.

II. EXPERIMENT

A. Sample preparation

The thin-film sample was prepared by the pulsed-laser deposition (PLD) method. An ArF excimer laser with the wavelength of 193 nm (Lumonics: EX-748) was used as a light source. The ceramic target of the nominal composition was prepared by a solid-state reaction method. $SrTiO_3$ single-crystal wafer cut in a $\langle 100 \rangle$ orientation was used as the substrate. The size of the substrate was 10 mm square and 0.3 mm thick. The substrate temperature was approximately 600 °C during the deposition process. The distance between the target and substrate was set at 100 mm. Deposition was performed in an oxygen gas of 0.13 Pa irradiated by a low-pressure mercury lamp. The number of laser pulse shots required to yield a film thickness of 78 nm was 3×10^4. The film thickness was measured using inductively coupled plasma spectrometry. The film composition was the same as the nominal composition within the experimental error ($\sim5\%$) of the inductively coupled plasma spectrometry. After deposition, the film was kept in vacuum for half an hour and cooled at the rate of 20 °C/min. The background pressure was lower than 10^{-4} Pa.

B. X-ray-diffraction measurement

The sample was first analyzed by a two-circle x-ray diffractometer and by an x-ray precession camera using Cu $K\alpha$ radiation. The film was confirmed to consist of a single-phase infinite-layer compound, because no other peaks than those from both the infinite-layer compound and the substrate material were observed.

The integrated x-ray-diffraction intensity collection was carried out using four-circle diffractometers (RIGAKU AFC7R and AFC5R) using Cu $K\alpha$ radiation and Mo $K\alpha$ radiation. The x-ray beam was collimated to 0.5 mmϕ. The sample was cut into 3 mm square, attached on a glass capillary with epoxy, mounted on a eucentric goniohead in a direction so that the c axis of the film, which is perpendicular to the film surface, was accurately parallel to the ϕ axis of the diffractometer.

First, the setting parameters and cell constants for the $SrTiO_3$ substrate crystal were refined. Second, those for the film crystal were refined after the transformation of the setting parameters to the film crystal from the substrate crystal. Then the integrated intensities of Bragg spots from the film were measured. All spots in the reciprocal space upper the film surface (that is, h and k had both negative and positive values and l only positive), were collected. Redundant data were not removed. The conditions for the data collection are summarized in Table I and II.

C. Absorption correction for thin crystal

The absorption correction was carried out because the shape of the crystal was that of a thin plate. Figure 1 shows a schematic view of the sample setting. The data were collected in a symmetrical setting where the angle ω was half the angle 2θ. The difference from the conventional measurement for a small spherical single crystal is that the incident-beam size is always smaller than the area of the platelike crystal through the beam path when the following condition was satisfied. It is given by

$$\frac{D}{\sin\theta\sin\chi} < r \ , \tag{1}$$

where D is the diameter of the beam and r is a length of the sample along the beam direction. The projection of the incident beam upon the sample surface was ellipsoid elongated along the direction of the beam. It is required that the longer radius of the ellipsoid is smaller than the length of the sample. We used only the intensities of the spots to satisfy the above condition in the structure refinement. Most of the spots satisfied the above condition except for several low-angle spots in the measurement using Mo $K\alpha$ radiation.

TABLE I. Summary of crystallographic information for the $Sr_{0.875}Nd_{0.125}CuO_{2-\delta}$ thin crystal.

Dimensions (mm)	3×3×0.00008
Diffractometer	AFC-7R
Radiation	Cu $K\alpha$ (50 kV, 180 mA)
Monochromator	Graphite
Crystal system	Tetragonal
Space group	$P4/mmm$ (No. 123)
Z	1
Temperature	Ambient
Calculated density	5.96
Scan mode	$2\theta-\omega$
2θ range	3–137°
μ (cm^{-1})	630
Total reflection	164
Reflection used[a] ($I>3\sigma$)	116
Least squares	$\|F\|$
Data/parameter	14
R	0.0339
R_w	0.0458

[a]The number of reflections used for the refinement after removing the standard spots and the interfering spots from the observed spots.

TABLE II. Summary of crystallographic information for the $Sr_{0.875}Nd_{0.125}CuO_{2-\delta}$ thin crystal.

Dimensions (mm)	3×3×0.00008
Diffractometer	AFC-5R
Radiation	Mo $K\alpha$ (50 kV, 100 mA)
Monochromator	Graphite
Crystal system	Tetragonal
Space group	$P4/mmm$ (No. 123)
Z	1
Temperature	Ambient
Calculated density	5.96
Scan mode	$2\theta-\omega$
2θ range	0–120°
μ (cm^{-1})	342
Total reflection	1468
Reflection used[a] ($I>3\sigma$)	198
Least squares	$\|F\|$
Data/parameter	25
R	0.0544
R_w	0.0622

[a]The number of reflections used for the refinement after removing the standard spots and the interfering spots from the observed spots.

The intensity of the x ray through a material can be written in the following equation:

$$I_l = I_0 \exp(-\mu l) \ , \tag{2}$$

where I_l is the intensity of the x ray through a material, I_0 is the intensity of the incident x ray, μ is the absorption coefficient, and l is the length of the beam path in the crystal.

The intensity of the diffracted x ray of a certain spot for the thin crystal can be written as

$$I_d = \frac{K(\theta)S}{2\mu}|F|^2 A_t \ , \tag{3}$$

where I_d is the diffracted x-ray intensity, $K(\theta)$ is a factor including Lorenz and polarization factors, S is a cross section of the x-ray beam which is constant when the condition (1) is satisfied, $|F|$ is the absolute value of the

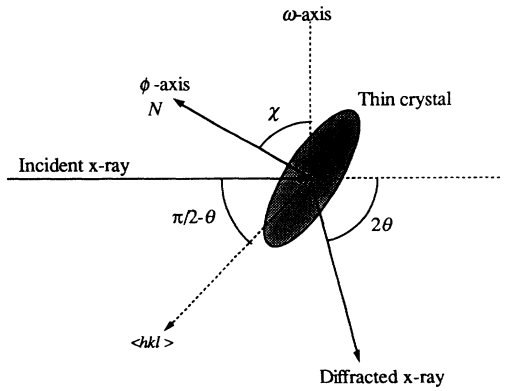

FIG. 1. Schematic view of sample setting in the four-circle diffractometer.

structure factor and A_t is the absorption correction factor.

A_t can be given by

$$A_t=\frac{\int_0^t I_l(t)dt}{\int_0^\infty I_l(t)dt} , \tag{4}$$

where t is the thickness of the crystal and $I_l(t)$ is I_l in formula (2) as a function of t.

Figure 2(a) shows a view of the cross section of the crystal perpendicular to the (hkl) plane and the ω axis. z is the thickness of the crystal along the beam path, which is written as

$$z=\frac{t}{\sin\chi} . \tag{5}$$

Figure 2(b) shows a view of the cross section of the crystal perpendicular to the incident x-ray beam and parallel to the ω axis. The length of the x-ray beam path, l, which is diffracted at the depth z, can be written as

$$l=\frac{2z}{\sin\theta}=\frac{2t}{\sin\theta\sin\chi} . \tag{6}$$

A_t can be calculated using formulas (2) and (4). Now A_t is written as

$$A_t=1-\exp\left[\frac{-2\mu t}{\sin\theta\sin\chi}\right] . \tag{7}$$

At last we corrected $|F|$ using formulas (3) and (7) for the structure refinement.

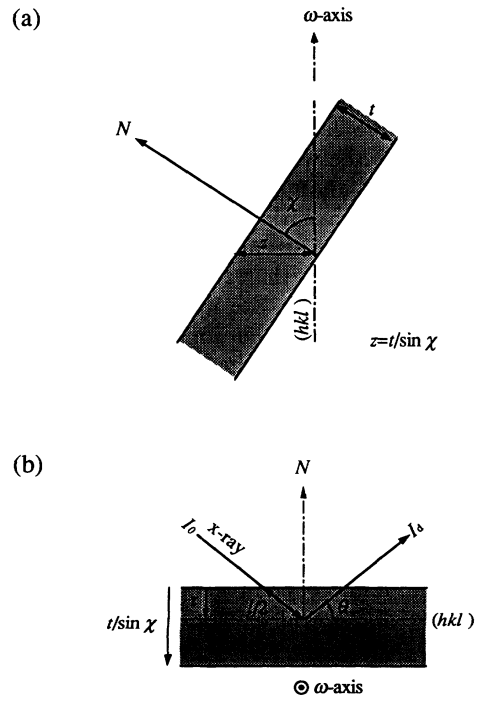

FIG. 2. (a) Cross-sectional view of the crystal perpendicular to the (hkl) plane and ω axis. (b) Cross-sectional view of the cross section of the crystal perpendicular to the x-ray beam and parallel to the ω axis.

D. Structure refinement

The crystal structure refinement was carried out using a TEXSAN program package (Molecular Structure Corporation). The least-square calculation based on the structure model was conducted on $|F|$ by a full matrix method. Anisotropic thermal parameters were refined in a final stage of the calculation.

Before the refinement, the collected data were carefully checked. First, we checked the superposition of the diffraction spots from the substrate material. In the data obtained by the measurement using Mo $K\alpha$ radiation, we removed several spots which were interfered. Second, we removed spots containing zero-order index numbers such as $0kl$, $h0l$, or $00l$. This is because these spots have a possibility of interference from Sr_2CuO_3-type planar defects which were commonly observed by transmission electron microscopy on the infinite-layer $SrCuO_2$ thin films.[5,6] For the film of (Sr,Nd)CuO_2, such defects have been similarly observed. The schematic view of the insertion of the defects between the matrix are shown in Fig. 3. The a-axis lengths of the matrix ($SrCuO_2$) and the defect (Sr_2CuO_3) have almost the same values, and the c-axis length of the matrix and b-axis length of the defect are almost the same. Therefore, the above-mentioned spots might contain information from the defect crystallites. As a result of the removal of the interfering spots, the data measured using Cu $K\alpha$ radiation mainly contained low-angle spots, and the data measured using Mo $K\alpha$ radiation mainly contained high-angle spots.

III. RESULTS

A. Physical properties of the film

The x-ray precession photograph and preliminary scan by the four-circle diffractometer revealed that the film contained only the infinite-layer phase except for the defect. No orthorhombic distortion or structural modulation was observed.

The electrical resistivity of the film at room temperature was 6×10^{-4} Ω cm. With decreasing temperature, the resistivity increased and the superconducting transition was observed around 20 K. The sign of the thermoelectric power of the film was negative throughout the

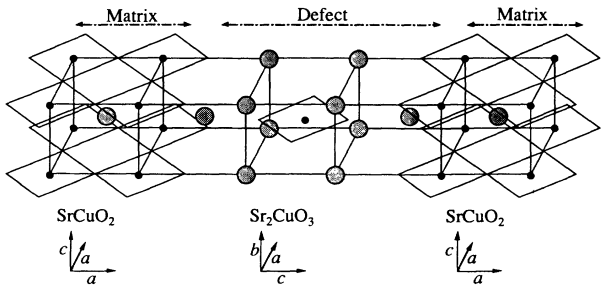

FIG. 3. Schematic view of the insertion of the defect crystals (Sr_2CuO_3) between the matrix crystals ($SrCuO_2$). Sr ions are represented as large hatched circles, Cu ions as small filled circles, and CuO_2 sheets as squares.

measured temperature range between 10 and 320 K. These data were presented in a previous paper.[7]

B. Crystal structure of the film

The determined atomic parameters with anisotropic thermal parameters are shown in Tables III and IV.

We successfully finished the refinement reducing discrepancy factors (R) down to 0.034 and 0.054 with the collected intensity data for Cu $K\alpha$ and Mo $K\alpha$ radiation, respectively. Observed structure factors (F_0) and calculated values (F_c) are listed in Tables V and VI. The difference between F_0 and F_c was small compared with the standard deviation of the observed structure factor (σF). In the space group $P4/mmm$, the Cu-O coordination is square planar. Occupation factors for Sr, Nd, and O ions were slightly smaller than the expected value from the nominal composition. Thermal parameters of Sr, Nd, and Cu ions were elongated in the c direction.

IV. DISCUSSION

A. Site occupancies and anisotropic thermal parameters

In general, strong correlation exists between occupation and thermal factors in the refinements. As the standard deviation of the data obtained by the measurement using Cu $K\alpha$ radiation were smaller than those obtained using Mo $K\alpha$ radiation, we employed the value refined from the data obtained using Cu $K\alpha$ radiation as occupation factors.

It is thought that the slight deficiency of Sr and Nd ions were due to the defect formation. As the average composition of the film was stoichiometric within the experimental error, the occupancy of the A-site cation in the matrix compound (infinite layer) occurred when $SrCuO_3$-type defects were formed. In the refinement of the occupation factor of oxygen, a much smaller value than 0.97 leads to unreasonable temperature factors.

TABLE III. (a) Crystallographic data for $Sr_{0.875}Nd_{0.125}CuO_{2-\delta}$ thin crystal. The radiation is Cu $K\alpha$; tetragonal cell, space group $P4/mmm$ (No. 123); $Z=1$; $a=3.920$ (1) Å; and $c=3.419$ (1) Å. (b) Anisotropic thermal parameters of $Sr_{0.875}Nd_{0.125}CuO_{2-\delta}$. Constraints: $u_{11}=u_{22}$ for Sr, Nd, and Cu. u_{ij} for Nd is equal to that for Sr. $u_{12}=u_{13}=u_{23}=0$ for all atoms.

Atom	Position	x	y	z	B_{eq} (Å^2)	g
			(a)			
Sr	1d	$\frac{1}{2}$	$\frac{1}{2}$	$\frac{1}{2}$	1.07 (5)	0.869
Nd	1d	$\frac{1}{2}$	$\frac{1}{2}$	$\frac{1}{2}$	1.01	0.117
Cu	1a	0	0	0	0.92 (7)	1.0 (fixed)
O	2f	$\frac{1}{2}$	0	0	1.0 (2)	0.97

Atom	u_{11}	u_{22}	u_{33}	u_{12}	u_{13}	u_{23}
			(b)			
Sr,Nd	0.0122(8)	0.0122	0.016(1)	0	0	0
Cu	0.008(1)	0.008	0.019(2)	0	0	0
O	0.010(2)	0.003(2)	0.027(2)	0	0	0

TABLE IV. (a) Crystallographic data for $Sr_{0.875}Nd_{0.125}CuO_{2-\delta}$ thin crystal. Radiation is Mo $K\alpha$; tetragonal cell, space group $P4/mmm$ (No. 123); $Z=1$; $a=3.9177$ (6) Å, and $c=3.4181$ (4) Å. (b) Anisotropic thermal parameters of $Sr_{0.875}Nd_{0.125}CuO_{2-\delta}$. Constraints: $u_{11}=u_{22}$ for Sr, Nd, and Cu. u_{ij} for Nd is equal to that for Sr. $u_{12}=u_{13}=u_{23}=0$ for all atoms.

Atom	Position	x	y	z	B_{eq} (Å^2)	g
			(a)			
Sr	1d	$\frac{1}{2}$	$\frac{1}{2}$	$\frac{1}{2}$	0.59(5)	0.869
Nd	1d	$\frac{1}{2}$	$\frac{1}{2}$	$\frac{1}{2}$	0.59	0.117
Cu	1a	0	0	0	0.68(7)	1.0(fixed)
O	2f	$\frac{1}{2}$	0	0	1.0(3)	0.97

Atom	u_{11}	u_{22}	u_{33}	u_{12}	u_{13}	u_{23}
			(b)			
Sr,Nd	0.0032(7)	0.0032	0.016(1)	0	0	0
Cu	0.007(1)	0.007	0.011(1)	0	0	0
O	0.014(5)	0.004(3)	0.019(4)	0	0	0

Therefore, it is reasonable to deduce that the oxygen content is not less than 0.97. The average copper valence calculated from the occupation factors was 1.77. From this value, the type of charge carriers are expected to be electrons. This is consistent with results for the thermoelectric-power measurement.[7]

The anisotropic thermal parameters of Sr, Nd, and Cu ions were elongated in the c direction. Inadequate absorption correction would lead to unusual anisotropic thermal parameters. In the present case, the difference in the anisotropy was very small between results employing two different wavelengths. Therefore, the anisotropy is thought to be intrinsic. The absolute values of the thermal parameters were different between two results. This is because the calculated electron density distribution is changed by the wavelength of the x-ray due to the difference of the anomalous dispersion terms. The elongation of the thermal parameters along the c direction indicates that the strength of the bond along this direction is weaker than that along the a or b direction. On infinite-layer cuprates, the main feature is the complete lack of the apical oxygen ion, which is a key result of the two dimensionality of the crystal and the weakness of the bond along the c direction.

B. Apical oxygen and the planarity of the CuO_2 sheets

It is important to investigate the coordination of oxygen ions around the copper ion in the study of the cuprate superconductors. We investigated the possibility of the existence of the apical oxygen ion. When we placed some small amount of oxygen in the apical (1b) site, one component of the anisotropic thermal factor of oxygen went to the negative value. Thus we concluded that the apical oxygen does not exist in the crystal.

The planarity of CuO_2 sheets is also an important feature in this crystal. Billinge *et al.*[8] reported deviations from the planarity of CuO_2 sheets in

TABLE V. Structure factors of observed reflections and calculated values (Cu $K\alpha$). F_0: observed structure factor; F_c: calculated structure factor; $\sigma(F)$: standard deviation of observed structure factor.

h	k	l	F_0	F_c	$\sigma(F)$	h	k	l	F_0	F_c	$\sigma(F)$
−1	−1	1	181	180	5	1	−2	2	76	73	2
−1	1	1	180	180	5	1	2	2	75	73	2
1	−1	1	182	180	5	−1	−3	2	227	215	7
1	1	1	181	180	5	−1	3	2	225	215	7
−1	−2	1	387	390	11	1	−3	2	228	215	7
−1	2	1	386	390	11	1	3	2	225	215	7
1	−2	1	388	390	11	−1	−4	2	59	57	2
1	2	1	390	390	11	−1	4	2	58	57	2
−1	−3	1	110	115	3	1	−4	2	59	57	2
−1	3	1	110	115	3	1	4	2	58	57	2
1	−3	1	111	115	3	−2	−1	2	75	73	2
1	3	1	110	115	3	−2	1	2	75	73	2
−1	−4	1	227	228	7	2	−1	2	76	73	2
−1	4	1	225	228	7	2	1	2	76	73	2
1	−4	1	226	228	7	−2	−2	2	332	310	10
1	4	1	227	228	7	−2	2	2	328	310	10
−2	−1	1	388	390	11	2	−2	2	334	310	10
−2	1	1	375	390	11	2	2	2	332	310	10
2	−1	1	388	390	11	−2	−3	2	67	60	2
2	1	1	392	390	11	−2	3	2	66	60	2
−2	−2	1	22	23	1	2	−3	2	67	60	2
−2	2	1	22	23	1	2	3	2	66	60	2
2	−2	1	23	23	1	−3	−1	2	227	215	7
2	2	1	23	23	1	−3	1	2	225	215	7
−2	−3	1	259	270	8	3	−1	2	227	215	7
−2	3	1	254	270	7	3	1	2	228	215	7
2	−3	1	258	270	8	−3	−2	2	67	60	2
2	3	1	260	270	8	−3	2	2	66	60	2
−2	−4	1	25	26	1	3	−2	2	67	60	2
−2	4	1	25	26	1	3	2	2	67	60	2
2	−4	1	26	26	1	−4	−1	2	58	57	2
2	4	1	25	26	1	−4	1	2	59	57	2
−3	−1	1	110	115	3	4	−1	2	60	57	2
−3	1	1	108	115	3	4	1	2	59	57	2
3	−1	1	111	115	3	−1	−1	3	98	101	3
3	1	1	111	115	3	−1	1	3	99	101	3
−3	−2	1	261	270	8	1	−1	3	96	101	3
−3	2	1	253	270	7	1	1	3	97	101	3
3	−2	1	259	270	8	−1	−2	3	216	223	6
3	2	1	262	270	8	−1	2	3	215	223	6
−3	−3	1	87	91	3	1	−2	3	217	223	6
−3	3	1	84	91	2	1	2	3	215	223	6
3	−3	1	86	91	2	−1	−3	3	79	81	2
3	3	1	87	91	3	−1	3	3	78	81	2
−4	−1	1	229	228	7	1	−3	3	81	81	2
−4	1	1	226	228	7	1	3	3	80	81	2
4	−1	1	230	228	7	−2	−1	3	217	223	6
4	1	1	230	228	7	−2	1	3	214	223	6
−4	−2	1	26	26	1	2	−1	3	216	223	6
−4	2	1	26	26	1	2	1	3	216	223	6
4	−2	1	26	26	1	−2	−2	3	35	37	1
4	2	1	25	26	1	−2	2	3	34	37	1
−1	−1	2	314	302	9	2	−2	3	34	37	1
−1	1	2	313	302	9	2	2	3	35	37	1
1	−1	2	315	302	9	−3	−1	3	80	81	2
1	1	2	314	302	9	−3	1	3	80	81	2
−1	−2	2	76	73	2	3	−1	3	80	81	2
−1	2	2	76	73	2	3	1	3	80	81	2

TABLE VI. Structure factors of observed reflections and calculated values (Mo $K\alpha$). F_0: observed structure factor; F_c: calculated structure factor; $\sigma(F)$: standard deviation of observed structure factor.

h	k	l	F_0	F_c	$\sigma(F)$	h	k	l	F_0	F_c	$\sigma(F)$
−1	−1	2	327	329	10	5	7	2	80	84	8
−1	1	2	335	329	10	−6	−2	2	170	167	8
1	−1	2	330	329	10	−6	2	2	189	167	9
1	1	2	330	329	10	6	−2	2	157	167	9
−1	−2	2	57	52	4	6	2	2	173	167	8
−1	2	2	48	52	5	−6	−6	2	106	104	7
1	−2	2	60	52	4	−6	6	2	85	104	8
1	2	2	62	52	4	6	−6	2	102	104	7
−1	−3	2	261	255	8	6	6	2	110	104	6
−1	3	2	244	255	8	−7	−1	2	121	114	6
1	−3	2	272	255	8	−7	1	2	130	114	7
1	3	2	251	255	8	7	−1	2	132	114	7
−1	−5	2	178	175	8	7	1	2	122	114	6
−1	5	2	165	175	8	−7	−3	2	99	102	7
1	5	2	172	175	8	−7	3	2	93	102	8
−1	−7	2	109	114	7	7	−3	2	96	102	8
−1	7	2	116	114	7	7	3	2	113	102	7
1	−7	2	117	114	7	−7	−5	2	77	84	8
1	7	2	116	114	7	−7	5	2	74	84	9
−2	−1	2	54	52	4	7	−5	2	74	84	9
−2	1	2	49	52	4	7	5	2	84	84	8
2	−1	2	50	52	4	−8	−2	2	104	110	7
2	1	2	55	52	4	−8	2	2	105	110	7
−2	−2	2	364	349	11	8	−2	2	116	110	6
−2	2	2	364	349	11	8	2	2	116	110	6
2	−2	2	365	349	11	−1	−1	3	75	74	5
2	2	2	363	349	11	−1	1	3	68	74	6
−2	−3	2	48	53	6	1	−1	3	74	74	5
2	−3	2	52	53	6	1	1	3	68	74	6
2	3	2	49	53	6	−1	−2	3	248	257	9
−2	−6	2	175	167	8	−1	2	3	236	257	10
−2	6	2	152	167	8	1	−2	3	252	257	9
2	−6	2	166	167	8	1	2	3	232	257	10
2	6	2	181	167	10	−1	3	3	57	67	9
−2	−8	2	121	110	6	−1	−4	3	184	189	10
−2	8	2	115	110	6	−1	4	3	178	189	8
2	−8	2	105	110	7	1	−4	3	197	189	9
2	8	2	114	110	6	1	4	3	182	189	10
−3	−1	2	265	255	8	−1	−6	3	126	128	8
−3	1	2	268	255	8	−1	6	3	112	128	9
3	−1	2	260	255	8	1	−6	3	111	128	9
3	1	2	261	255	8	1	6	3	119	128	8
−3	−2	2	44	53	7	−2	−1	3	245	257	10
3	−2	2	48	53	6	−2	1	3	243	257	10
−3	−3	2	220	208	9	2	−1	3	253	257	9
−3	3	2	211	208	9	2	1	3	250	257	9
3	−3	2	209	208	9	−2	−3	3	197	210	9
3	3	2	215	208	9	−2	3	3	184	210	9
−3	−7	2	113	102	7	2	−3	3	196	210	9
−3	7	2	84	102	8	2	3	3	200	210	9
3	−7	2	106	102	7	−2	−5	3	141	153	8
3	7	2	115	102	7	−2	5	3	145	153	8
−5	−1	2	178	175	8	2	−5	3	136	153	7
−5	1	2	163	175	8	2	5	3	147	153	8
5	−1	2	197	175	11	3	−1	3	69	67	8
5	1	2	175	175	8	3	1	3	61	67	9
−5	−7	2	79	84	8	−3	−2	3	197	210	9
−5	7	2	85	84	8	−3	2	3	194	210	9
5	−7	2	74	84	8	3	−2	3	195	210	9

TABLE VI. (*Continued*).

h	k	l	F_0	F_c	$\sigma(F)$	h	k	l	F_0	F_c	$\sigma(F)$
3	2	3	201	210	9	−2	4	4	173	149	9
−3	−4	3	154	161	8	2	−4	4	171	149	9
−3	4	3	149	161	8	2	4	4	154	149	8
3	−4	3	150	161	8	−2	−6	4	110	108	13
3	4	3	166	161	8	−2	6	4	128	108	11
−4	−1	3	197	189	10	2	−6	4	114	108	12
−4	1	3	180	189	8	−3	−1	4	152	146	8
4	−1	3	186	189	10	−3	1	4	155	146	8
4	1	3	203	189	9	3	−1	4	132	146	8
−4	−3	3	147	161	7	3	1	4	150	146	8
−4	3	3	160	161	8	−3	−3	4	127	125	9
4	−3	3	155	161	8	−3	3	4	131	125	9
4	3	3	146	161	8	3	−3	4	127	125	9
−5	−2	3	148	153	8	3	3	4	106	125	11
−5	2	3	133	153	7	−4	−2	4	152	149	8
5	−2	3	147	153	8	−4	2	4	157	149	9
5	2	3	138	153	7	4	−2	4	149	149	8
−5	−6	3	87	92	12	4	2	4	159	149	9
−5	6	3	106	92	10	−4	−4	4	130	121	11
5	−6	3	92	92	11	−4	4	4	122	121	11
5	6	3	98	92	10	4	−4	4	133	121	11
−6	−1	3	132	128	8	4	4	4	129	121	11
−6	1	3	127	128	8	−6	2	4	95	108	15
6	−1	3	124	128	8	6	−2	4	108	108	13
−6	−5	3	86	92	12	6	2	4	121	108	12
−6	5	3	96	92	11	−1	−2	5	126	125	11
6	−5	3	101	92	10	−1	2	5	130	125	11
−1	−1	4	175	175	9	1	−2	5	136	125	10
−1	1	4	181	175	9	1	2	5	129	125	11
1	−1	4	190	175	9	−2	−1	5	129	125	11
1	1	4	182	175	9	−2	1	5	118	125	12
−1	−3	4	156	146	8	2	−1	5	139	125	10
−1	3	4	142	146	8	2	1	5	123	125	11
1	−3	4	152	146	8	−2	−3	5	96	108	16
1	3	4	167	146	9	−2	3	5	104	108	15
−2	−2	4	198	190	10	2	−3	5	102	108	15
−2	2	4	207	190	10	−3	−2	5	105	108	15
2	−2	4	199	190	10	−3	2	5	101	108	15
2	2	4	192	190	10	3	−2	5	99	108	15
−2	−4	4	158	149	8	3	2	5	112	108	14

$Ca_{0.85}Sr_{0.15}CuO_2$. They observed uncorrelated displacements of oxygen atoms along the c direction within a deviation of 0.1 Å. In the present study, we assumed random displacements of oxygen ($4i$ site) because no orthorhombic distortion or structural modulation was observed. When the value z is smaller than 0.015 (0.05 Å), there is no remarkable change in the R factor. When the value z is increased larger than this value, the R factor gradually increases. Therefore, it is concluded that the CuO_2 sheets are square planar with a deviation of less than 0.05 Å.

V. CONCLUSION

The crystal structure of the $Sr_{0.875}Nd_{0.125}CuO_{2-\delta}$ thin film was analyzed by an x-ray four-circle diffraction method. The film was grown on a $SrTiO_3$ substrate by the pulsed-laser deposition technique. It was confirmed that the film consists of a single phase of the infinite-layer compound. No orthorhombic distortion or structural modulation was observed. The crystal had a tetragonal cell, the lattice constants are $a=3.92$ Å and $c=3.42$ Å with the space group $P4/mmm$. The absorption correction for a thin platelike crystal leads to success in the structure refinement. The copper-oxygen sheet was a square plane without buckling, whose deviation was less than 0.05 Å, and no apical oxygen ion was coordinated. Sr and Nd ions were slightly deficient from the nominal value because of Sr_2CuO_3 type defect formation. Anisotropic thermal parameters of Sr, Nd, and Cu ions were elongated along the c direction, indicating the crystallographic two dimensionality of the infinite-layer structure.

ACKNOWLEDGMENTS

The authors wish to express their thanks to Toshihiko Hori and Mikio Yamasaki of RIGAKU Corporation for their help in the absorption correction and part of the measurement. They also thank Koichi Kubo, Kenji Nakanishi, and Kiyoshi Yamamoto of the Superconductivity Research Laboratory for their helpful discussions. This work was supported by the New Energy and Industry Technology Development Organization for the Research and Development of Industrial Science and Technology Frontier Program.

[1]T. Siegrist, S. M. Zahurak, D. W. Murphy, and R. S. Roth, Nature **334**, 231 (1988).

[2]M. G. Smith, A. Manthiram, J. Zhou, J. B. Goodenough, and J. T. Markert, Nature **351**, 549 (1991).

[3]H. Adachi, T. Satoh, Y. Ichikawa, K. Setsune, and K. Wasa, Physica C **196**, 14 (1992).

[4]N. Sugii, K. Kubo, M. Ichikawa, K. Yamamoto, H. Yamauchi, and S. Tanaka, Jpn. J. Appl. Phys. **31**, L1024 (1992).

[5]S. Takeno, S. Nakamura, Y. Terashima, and T. Miura, Physica C **206**, 75 (1993).

[6]N. Sugii, M. Ichikawa, K. Hayashi, K. Kubo, K. Yamamoto, and H. Yamauchi, Physica C **213**, 345 (1993).

[7]N. Sugii, K. Matsuura, K. Kubo, K. Yamamoto, M. Ichikawa, and H. Yamauchi, J. Appl. Phys. **74**, 4047 (1993).

[8]S. J. L. Billinge, P. K. Davies, T. Egami, and C. R. A. Catlow, Phys. Rev. B **43**, 10 340 (1991).

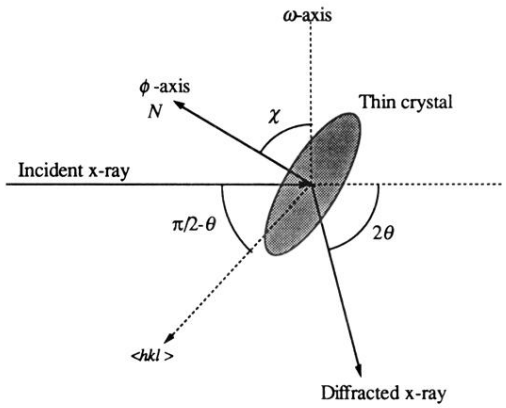

FIG. 1. Schematic view of sample setting in the four-circle diffractometer.

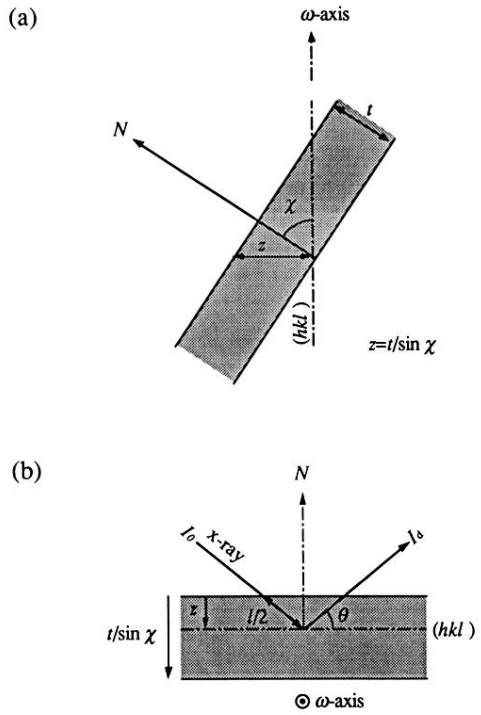

FIG. 2. (a) Cross-sectional view of the crystal perpendicular to the (hkl) plane and ω axis. (b) Cross-sectional view of the cross section of the crystal perpendicular to the x-ray beam and parallel to the ω axis.

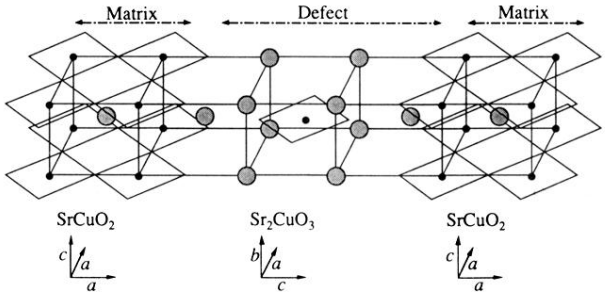

FIG. 3. Schematic view of the insertion of the defect crystals (Sr_2CuO_3) between the matrix crystals ($SrCuO_2$). Sr ions are represented as large hatched circles, Cu ions as small filled circles, and CuO_2 sheets as squares.